Journal of Alloys and Compounds 502 (2010) 211–214

Contents lists available at ScienceDirect

Journal of Alloys and Compounds

journal homepage: www.elsevier.com/locate/jallcom

Subsolidus phase relations and the crystallization region of $LiNbO_3$ in the system $Li_2O–B_2O_3–Nb_2O_5$

Can Huang, Shichao Wang, Ning Ye*

Key Laboratory of Optoelectronic Materials Chemistry and Physics, Fujian Institute of Research on the Structure of Matter, Chinese Academy of Sciences, Fuzhou, Fujian 350002, PR China

ARTICLE INFO

Article history:
Received 10 February 2010
Received in revised form 15 April 2010
Accepted 17 April 2010
Available online 21 May 2010

Keywords:
Lithium niobate
Crystal growth
Phase diagrams
Borate
Thermal analysis

ABSTRACT

Subsolidus phase relations in ternary system $Li_2O–B_2O_3–Nb_2O_5$ were determined and its phase diagram was constructed with the aid of XRD analysis. Eleven three-phase regions were identified in the subsolid phase diagram while no ternary compound was found. Meanwhile, four pseudo-binary systems, i.e., $LiNbO_3–LiB_3O_5$, $LiNbO_3–Li_2B_4O_7$, $LiNbO_3–LiBO_2$, and $LiNbO_3–Li_3B_2O_{4.5}$, were investigated and partial phase diagrams were determined on the $LiNbO_3$-rich side. Finally, the crystallization region of $LiNbO_3$ was identified in the ternary phase diagram. $LiNbO_3$ crystals can be grown by using a lithium borate as the flux below 1100 °C.

© 2010 Elsevier B.V. All rights reserved.

1. Introduction

$LiNbO_3$ (LN) is a typical non-stoichiometric material melting congruently with a composition of 48.6 mol% Li_2O. It is usually grown by the Czochralski method at this congruent point [1]. However, due to Li deficiency, the LN crystals grown by the Congruent-Czochralski method (CLN) turn out to possess non-ignorable intrinsic defects, mainly Nb_{Li} and V_{Li}. These intrinsic defects impose serious influences on LN physical properties and thus limit its technical applications.

Efforts have been directed to preparing stoichiometric LN (SLN) by employing different methods including growth or post-growth processing techniques in order to increase the Li/Nb ratio. It is difficult to grow a homogeneous bulk crystal from a Li-rich (55–60 mol% Li) melt by using the conventional Czochralski method due to the segregation effect [2,3]. To circumvent this difficulty, a continuous charging Czochralski method has been proposed by Kan et al. It was further modified by Kitamura et al. [4,5] that led to the development of the double crucible Czochralski Method, by which a Ø 40 mm × (50–100) mm SLN with the lithium concentration 49.6–49.9 mol% has been successfully grown. Adding alkaline additives such as K_2O or Cs_2O into the melt were proved to be beneficial for SLN crystallizing [6–12]. In addition, the vapor transport equilibration technique has been developed to change the Li/Nb ratio, by which a near-stoichiometric LN (49.9 mol% Li) [13–16] can be obtained for thin crystal samples. Meanwhile, the flux method was utilized to grow LN thick layers and small crystallites using $LiVO_3$ as the flux. The drawback of this solvent is that the V^{5+} ions reside in the crystal and render it weakly green colored. Lithium borate is widely employed as the flux due to its good dissolvability, low melting temperature, and the benefit against transition metal contamination. Detailed phase relations involving lithium borate are usually required for crystallization. However, to date, the phase relations of the ternary system $Li_2O–B_2O_3–Nb_2O_5$ are scarcely reported.

The binary system $Li_2O–B_2O_3$ has been studied by many groups and its phase diagram has been well constructed [17–22]. Several compounds, including congruently melting $Li_2O{\cdot}B_2O_3$, $Li_2O{\cdot}2B_2O_3$, and incongruently melting $2Li_2O{\cdot}5B_2O_3$, $Li_2O{\cdot}3B_2O_3$ and $Li_2O{\cdot}4B_2O_3$, have been identified and reported. In addition, the lithium-rich region was investigated by Maraine-Giroux et al. [21] and Bouaziz and Maraine [22]. The compounds $Li_3B_2O_{4.5}$, $Li_4B_2O_5$, and Li_3BO_3 have been determined based on their work.

The phase relation of $Li_2O–Nb_2O_5$ has also been extensively investigated [23–28]. Five compounds, i.e., $Li_2Nb_{28}O_{71}$, $Li_2Nb_8O_{21}$, $LiNb_3O_8$, $LiNbO_3$, and Li_3NbO_4 have been identified [23]. Meanwhile, a solid-solution range extending from 44 mol% to 50.5 mol% Li_2O as well as a congruently melting composition at 48.5 mol% Li_2O in $LiNbO_3$ has been found by Lerner et al. [24].

The phase relationship of $B_2O_3–Nb_2O_5$ had been reported by Levin [29]; however, only compound Nb_3BO_9 has been found.

Two ternary compounds, i.e., $Li_6Nb_4B_6O_{22}$ and $Li_2Nb_4B_2O_{14}$, have been reported in the study of the pseudo-binary system $LiBO_2–Nb_2O_5$ [30], and the unindexed X-ray powder diffraction

---

* Corresponding author. Fax: +86 591 83776076.
E-mail address: nye@fjirsm.ac.cn (N. Ye).

0925-8388/$ – see front matter © 2010 Elsevier B.V. All rights reserved.
doi:10.1016/j.jallcom.2010.04.146

Table 1
The results of subsolidus phase identifications in the Li_2O–B_2O_3–Nb_2O_5 system.

Li_2O (mol%)	B_2O_3 (mol%)	Nb_2O_5 (mol%)	Condition	Phase analysis	Equivalent composition
0	25	75	800 °C, 72 h	Nb_3BO_9	Nb_3BO_9
7	18	75	700 °C, 72 h	$LiNb_3O_8 + Nb_3BO_9$	
10	10	80	720 °C, 72 h	$LiNb_3O_8 + Nb_3BO_9 + Nb_2O_5$	
10	40	50	850 °C, 72 h	$LiNb_3O_8 + Nb_3BO_9$	
20	30	50	850 °C, 72 h	$LiNb_3O_8 + B_2O_3$	
25	25	50	700 °C, 72 h	$LiNb_3O_8 + LiB_3O_5$	"$Li_2Nb_4B_2O_{14}$"
25	50	25	750 °C, 48 h	$LiNb_3O_8 + LiB_3O_5$	
26.7	56.7	16.6	750 °C, 48 h	$LiNb_3O_8 + LiB_3O5 + Li_2B_4O_7$	
28.5	71.5	0	650 °C, 72 h	$Li_2B_4O_7 + LiB_3O_5$	
31.3	56.2	12.5	800 °C, 60 h	$LiNbO_3 + LiNb_3O_8 + Li_2B_4O_7$	$LN{:}LiB_3O_5 = 4{:}6$
35.7	42.9	21.4	830 °C, 65 h	$LiNbO_3 + Li_2B_4O_7 + LiNb_3O_8$	$LN{:}LiB_3O_5 = 6{:}4$
37.5	37.5	25	700 °C, 72 h	$LiNbO_3 + Li_2B_4O_7 + LiNb_3O_8$	"$Li_6Nb_4B_6O_{22}$"
40	50	10	720 °C, 72 h	$LiNbO_3 + Li_2B_4O_7 + LiBO_2$	
40.6	37.5	21.9	820 °C, 55 h	$LiNbO_3 + Li_2B_4O_7$	$LN{:}Li_2B_4O_7 = 7{:}3$
45.5	13.6	40.9	830 °C, 65 h	$LiNbO_3 + Li_2B_4O_7 + LiNb_3O_8$	$LN{:}LiB_3O_5 = 9{:}1$
45.8	16.7	37.5	820 °C, 55 h	$LiNbO_3 + Li_2B_4O_7$	$LN{:}Li_2B_4O_7 = 9{:}1$
46.7	26.7	26.6	720 °C, 72 h	$LiNbO_3 + Li_2B_4O_7 + LiBO_2$	
46.7	36.7	16.6	720 °C, 72 h	$LiNbO_3 + Li_2B_4O_7 + LiBO_2$	
46.7	46.7	6.6	720 °C, 72 h	$LiNbO_3 + Li_2B_4O_7 + LiBO_2$	
50	10	40	750 °C, 55 h	$LiNbO_3 + LiBO_2$	$LN{:}LiBO_2 = 8{:}2$
50	30	20	750 °C, 48 h	$LiNbO_3 + LiBO_2$	$LN{:}LiBO_2 = 4{:}6$
50	40	10	800 °C, 55 h	$LiNbO_3 + LiBO_2$	$LN{:}LiBO_2 = 2{:}8$
52.2	8.7	39.1	750 °C, 65 h	$LiNbO_3 + Li_3NbO_4 + LiBO_2$	$LN{:}Li_3B_2O_{4.5} = 9{:}1$
55.2	20.7	24.1	750 °C, 65 h	$LiNbO_3 + Li_3NbO_4 + LiBO_2$	$LN{:}Li_3B_2O_{4.5} = 3{:}7$
57.21	14.29	28.5	700 °C, 45 h	$LiNbO_3 + Li_3NbO_4 + LiBO_2$	
58.5	34.1	7.4	750 °C, 65 h	$LiNbO_3 + Li_3NbO_4 + LiBO_2$	$LN{:}Li_3B_2O_{4.5} = 7{:}3$
63.3	23.3	13.4	650 °C, 48 h	$Li_3NbO_4 + LiBO_2$	
64.6	29.2	6.2	650 °C, 48 h	$Li_3NbO_4 + Li_3B_2O_{4.5}$	
69	21	10	650 °C, 72 h	$Li_3NbO_4 + Li_4B_2O_5$	
75	20	5	650 °C, 72 h	$Li_3NbO_4 + Li_3BO_3$	
80	15	5	600 °C, 48 h	$Li_3NbO_4 + Li_3BO_3$	

data of these two compounds have also been reported by the same authors. However, to the best of our knowledge, no phase relations of the compositions that extend over the entire Li_2O–B_2O_3–Nb_2O_5 ternary region have been reported. In this work, we report a study of subsolidus phase relations in ternary system Li_2O–B_2O_3–Nb_2O_5, and meanwhile, the crystallizations region for LN growth has also been identified.

2. Experimental procedures

A series of Li_2CO_3–Nb_2O_5–B_2O_3 samples with different ingredient compositions were prepared via solid-state reaction in air by using the mixtures of analytical grade Li_2CO_3, Nb_2O_5 and B_2O_3 as raw materials. The total weight of each mixture was about 2 g. The samples were ground in an agate mortar and heated in alumina crucibles below 850 °C in a muffle furnace for different heat treatments accordingly upon different compositions as listed in Table 1. The heating temperatures in the Li-rich region were usually lower. The samples were then cooled to room temperature with a rate of 20 K/h. Phase identification of the samples was carried out on a PANalytical X'Pert Prodiffractometer with CuKα radiation (45 kV × 40 mA) using continuous mode at a rate of $2\theta = 5°$/min. The process was repeated several times until the X-ray pattern of a specimen showed no further change upon successive heat treatments.

The partial phase diagrams of pseudo-binary system LN–LiB_3O_5, LN–$Li_2B_4O_7$, LN–$LiBO_2$, and LN–$Li_3B_2O_{4.5}$ were constructed based on the differential thermal analysis data collected from a NETZSCH DTA 404PC apparatus in platinum crucibles with a heating rate of 10 K/min. The measurements were performed in a nitrogen atmosphere in the temperature range of 20–1150 °C with α-Al_2O_3 as the reference. There were two endothermal peaks on each heating curve. The onset temperature of the first endothermal peak was determined as the eutectic temperature, while the end temperature of the second one was determined as the liquid-solid coexistence temperature. All borates and LN used in the differential thermal analysis were prepared prior to measurements through solid-state reactions.

Spontaneous nucleation method was employed to determine the crystallization condition of LN crystals. The solutions were prepared in the Pt crucibles (diameter 30 mm, height 30 mm) by melting the mixtures of the starting compounds in appropriate ratios according to the compositions of the flux systems. The total amount of each melt varied between 5 g and 10 g, depending on the melt composition. A starting mixture was heated in the center of a vertical furnace equipped with an observation window at the top, until the melt became transparent and clear. Then it was held for 10 h at a temperature 20–50 °C higher than this observed saturation temperature, which was measured on the surface of the melt. The homogenized solution was subsequently cooled in steps of 10 °C after every 6 h until the crystals appeared in the melt. Thereafter, the whole melt was cooled down at a rate of 5 °C/h until sufficient amount crystals for further tests emerged. Finally, the melt was cooled in the air, and the crystals were isolated and identified using powder X-ray analysis.

3. Results and discussion

3.1. Subsolidus phase relationship of the system Li_2O–B_2O_3–Nb_2O_5

3.1.1. Binary systems

The experiments were conducted over the composition range from 1:3 to 3:1 in the Li_2O–B_2O_3 system. All compounds reported in the literature except for $Li_4B_{10}O_{17}$ have been observed in our experiments through XRD analysis. $Li_4B_{10}O_{17}$ transformed to LiB_3O_5 and

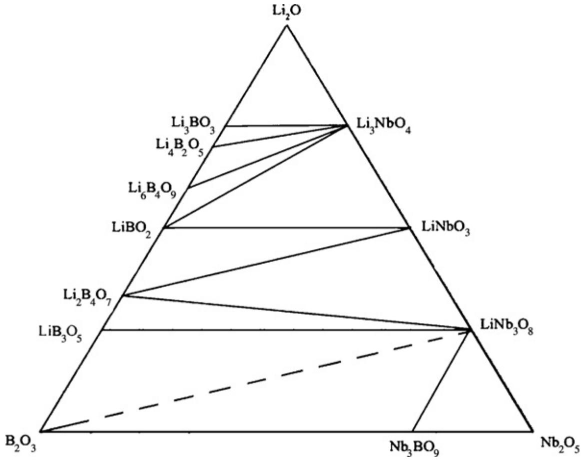

Fig. 1. Subsolidus phase relationships of the system Li_2O–B_2O_3–Nb_2O_5.

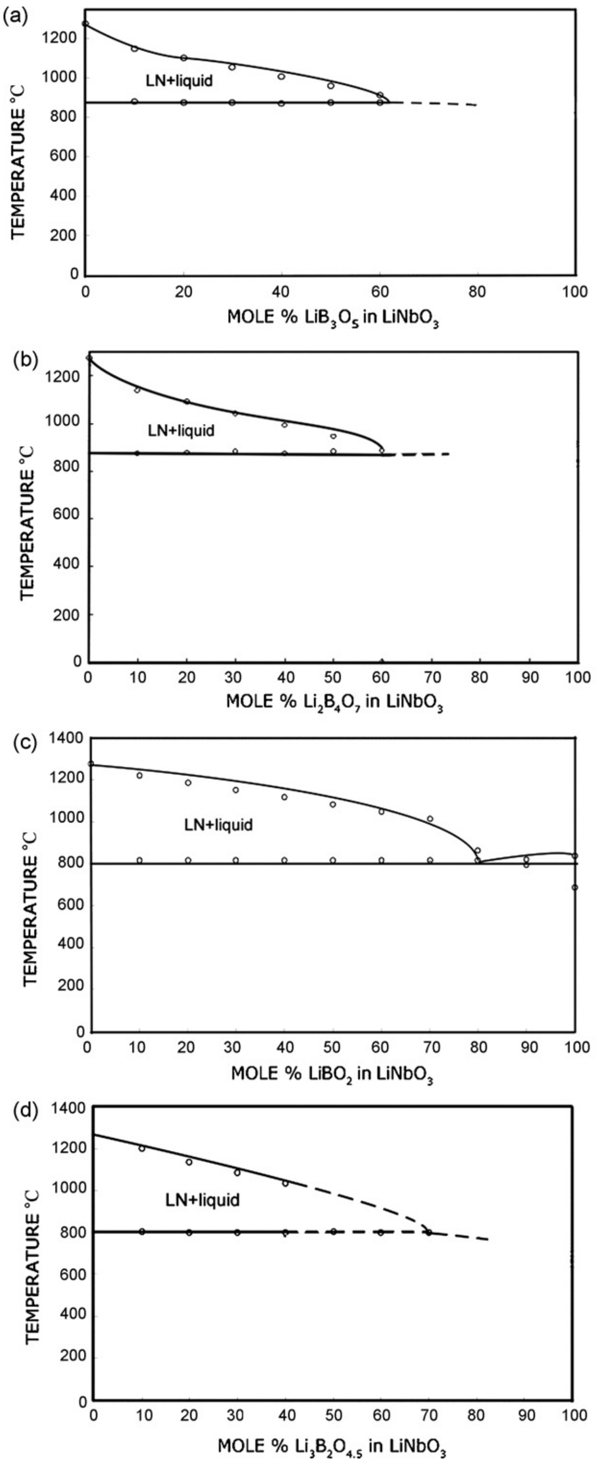

Fig. 2. Pseudo-binary diagrams (T-X, constant-pressure) of LN–LiB_3O_5 (a), LN–$Li_2B_4O_7$ (b), LN–$LiBO_2$ (c), LN–$Li_3B_2O_{4.5}$ (d).

$Li_2B_4O_7$ when the samples were slowly cooled down to room temperature, which is in agreement with the phase relations reported in Ref. [20]. All the compounds in binary system B_2O_3–Nb_2O_5 and Li_2O–Nb_2O_5 (Nb_2O_5:$Li_2O < 3$) were also found and confirmed by XRD analysis.

3.1.2. Ternary system

The phase identification (via XRD) results are summarized in Table 1, and the subsolidus phase relationships were established as shown in Fig. 1. Eleven three-phase regions were identified in the ternary system, however, no ternary compound was observed in current XRD analysis, which is similar to those in the Li_2O–B_2O_3–Ta_2O_5 system [31]. The ternary compound $Li_6Nb_4B_6O_{22}$ and $Li_2Nb_4B_2O_{14}$ reported in Ref. [30] were not found in this study. In order to verify the formation of these two ternary compounds, the solid-state reactions at these compositions were carried out. However, the XRD analysis results revealed that all the reaction products were a mixture of binary compounds as listed in Table 1. $Li_2Nb_4B_2O_{14}$ was actually the mixture of $LiNb_3O_8$ and LiB_3O_5 located at a two-phase boundary, while $Li_6Nb_4B_6O_{22}$ was the mixture of LN, $Li_2B_4O_7$ and $LiNb_3O_8$ located in a three-phase region. Moreover, the differential thermal analysis results also contradicted with the congruent melting behaviors of these two compositions as proposed in Ref. [30]. Only lithium niobate crystals could be obtained from the melts of these two compositions by using spontaneous nucleation method.

3.2. Pseudo-binary phase diagrams

The system LN–LiB_3O_5, LN–$Li_2B_4O_7$, LN–$LiBO_2$, and LN–$Li_3B_2O_{4.5}$ were investigated by means of XRD and DTA methods. Partial phase diagrams were constructed on the LN-rich side for these four pseudo-binary systems (Fig. 2). Due to the complicated phase relations in Li_2O–B_2O_3 system, the pseudo-binary diagrams at borate-rich sides were not completely resolved. However, as shown in Fig. 2, lithium borates exhibit remarkable solubility in LN at the temperatures below 1100 °C, and thus are suitable for crystal growth by flux method.

3.3. Crystallization zone of lithium niobate in the Li_2O–B_2O_3–Nb_2O_5

To better define the crystallization region of LN crystals, spontaneous nucleation method was employed to determine the monophase crystallization boundaries in the Li_2O–B_2O_3–Nb_2O_5 system. The concentration region of LN crystallization is comparatively wide as shown in Fig. 3, enclosed by lithium borate phase on the left side, Li_3NbO_4 on the upper side, and $LiNb_3O_8$ on the bottom side. The LN crystallization isotherms within the monophase region, as shown in Fig. 3, were estimated at an interval of 40 °C from 950 °C to 1110 °C based on the data from the psuedo-binary

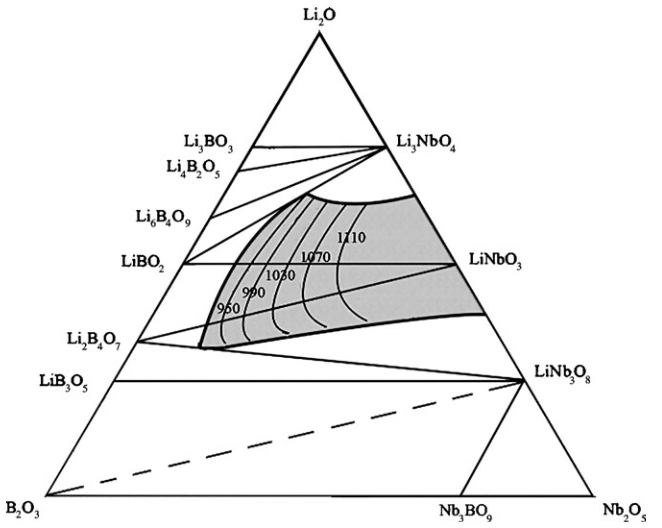

Fig. 3. The ternary Li_2O–B_2O_3–Nb_2O_5 system. Hatched area is the LN crystallization field.

Table 2
Selected sample compositions for LN crystallization as well as corresponding phase identifications in the Li_2O–B_2O_3–Nb_2O_5 system.

Li_2O (mol%)	B_2O_3 (mol%)	Nb_2O_5 (mol%)	Phase of initial crystallization
30	50	20	$LiNb_3O_8$
31.2	56.3	12.5	LN
35	40	25	LN
35	35	30	$LiNb_3O_8$
36.3	54.65	8.95	LN
37.3	50.9	11.8	LN
39	33	28	LN
40	40.3	19.7	LN
40.6	37.4	22	LN
50	37.5	12.5	LN
50	20	30	LN
54	15.8	30.2	LN
56.2	25	18.8	LN
58	32	10	LN
62.5	17.5	20	LN
65	15	20	Li_3NbO_4
65	17.75	17.75	Li_3NbO_4
65	20	15	LN

phase diagrams combined with those from spontaneous nucleation experiments. The selected sample compositions for LN crystallization as well as corresponding phase identifications are listed in Table 2.

4. Conclusions

The subsolidus phase relations of the ternary system Li_2O–B_2O_3–Nb_2O_5 were determined and the phase diagram was constructed by means of solid-state reaction and XRD analysis. There are eleven three-phase regions existing in the subsolidus phase diagram and no ternary compound was found in the present work. The pseudo-binary system LN–LiB_3O_5, LN–$Li_2B_4O_7$, LN–$LiBO_2$, and LN–$Li_3B_2O_{4.5}$ were investigated and partial phase diagrams were constructed on the LN-rich side. A wide crystallization region of LN was defined in the ternary phase diagram. Lithium borates with the compositions between $2Li_2O{\cdot}B_2O_3$ and $Li_2O{\cdot}3B_2O_3$ can be suitable fluxes for growing LN crystals below 1100 °C.

Acknowledgment

This study was supported by National Science Foundation of China (Grant No. 50872132, and 60608018).

References

[1] Ballmans AA, J. Am. Ceram. Soc. 48 (1965) 112.
[2] J.C. Bergman, A. Ashkin, A.A. Ballman, J.M. Dziedzic, H.J. Levinstein, R.G. Smith, Appl. Phys. Lett. 12 (1968) 92.
[3] S. Yao, J. Wang, H. Liu, X. Hu, H. Zhang, X. Cheng, Z. Ling, J. Alloys Compd. 455 (2008) 501–505.
[4] K. Kitamura, J.K. Yamamoto, N. Iyi, S. Kimura, T. Hayashi, J. Cryst. Growth 116 (1992) 327.
[5] S.J. Kan, M. Sakamoto, Y. Okano, K. Hoshikawa, T. Fukuda, J. Cryst. Growth 119 (1992) 215.
[6] G. Malovichko, V.G. Grachev, L.P. Yurchenko, V.Ya. Proshko, E.P. Kokanyan, V.T. Gabrielyan, Phys. Status Solidi A 133 (1992) K29.
[7] K. Polgár, A. Péter, L. Kovács, G. Corradi, Zs. Szaller, J. Cryst. Growth 177 (1997) 211.
[8] K. Polgár, Å. Péter, I. Földvári, Opt. Mater. 19 (2002) 7–11.
[9] G. Dravecz, B. Shackmann, M. Cochez1, M. Ferriol, J. Therm. Anal. Calorim. 90 (2007) 343–345.
[10] B. Lu, J. Xua, X. Li, G. Qian, Z. Xia, J. Alloys Compd. 449 (2008) 224–227.
[11] S. Zhang, H. Xia, J. Wang, Y. Zhang, J. Alloys Compd. 463 (2008) 446–452.
[12] A. Peter, K. Polgar, M. Ferriol, L. Poppl, I. Foldvari, M. Cochez, Z. Szaller, J. Alloys Compd. 386 (2005) 246–252.
[13] D.H. Jundt, M.M. Fejer, R.G. Norwood, P.F. Bordui, J. Appl. Phys. 72 (1992) 3468–3473.
[14] Y.S. Luh, M.M. Fejer, R.L. Byer, R.S. Feigelson, J. Cryst. Growth 85 (1987) 264.
[15] R.L. Holman, Mater. Sci. Res. 11 (1978) 343.
[16] P.F. Bordui, R.G. Norwood, D.H. Jundt, M.M. Fejer, J. Appl. Phys. 71 (1992) 875.
[17] A.P. Rollet, R. Bouaziz, Compt. Rend. 240 (1955) 2417.
[18] B.S.R. Sastry, F.A. Hummel, J. Am. Ceram. Soc. 41 (1958) 7.
[19] A.B. Kaplun, A.B. Meshalkin, J. Cryst. Growth 209 (2000) 890–894.
[20] B.S.R. Sastry, F.A. Hummel, J. Am. Ceram. Soc. 42 (1959) 216–218.
[21] G. Maraine-Giroux, R. Bouaziz, G. Perez, Rev. Chim. Miner. 9 (1972) 779.
[22] R. Bouaziz, G. Maraine, Compt. Rend. 274 (1972) 390.
[23] A. Reisman, F. Holtzberg, J. Am. Chem. Soc. 80 (1958) 6503–6507.
[24] P. Lerner, C. Legras, J.P. Dumas, J. Cryst. Growth 3/4 (1968) 231–235.
[25] R.S. Roth, H.S. Parker, W.S. Brower, J.L. Waring, Fast Ion Transport Solids (1973) 227.
[26] M. Lundberg, S. Andersson, Acta Chem. Scand. 19 (1965) 1376–1380.
[27] M. Lundberg, Acta Chem. Scand. 25 (1971) 3337–3346.
[28] B.M. Gatehouse, P. Leverett, Cryst. Struct. Commun. 1 (1972) 83–86.
[29] E.M. Levin, J. Res. Natl. Bur. Stand. Sect. A 70 (1966) 11–16.
[30] N.T. Buludov, F.D. Mamedaliev, Z.Sh. Karaev, G.K. Abdullaev, Zh. Neorg. Khim. 29 (1984) 1350–1351;
N.T. Buludov, F.D. Mamedaliev, Z.Sh. Karaev, G.K. Abdullaev, Russ. J. Inorg. Chem. (Engl. Transl.) 29 (1984) 770–771.
[31] G.M. Cai, W.Y. Wang, M. Li, Y.F. Lou, Y.P. Sun, X.L. Chen, Mater. Res. Bull. 44 (2009) 189–193.